International Journal of Mechanical, Industrial and Aerospace Sciences
ISSN: 2517-9950
Vol:7, No:12, 2013

Disturbance Observer-Based Predictive Functional Critical Control of a Table Drive System

Toshiyuki Satoh, Hiroki Hara, Naoki Saito, Jun-ya Nagase, Norihiko Saga

Abstract—This paper addresses a control system design for a table drive system based on the disturbance observer (DOB)-based predictive functional critical control (PFCC). To empower the previously developed DOB-based PFC to handle constraints on controlled outputs, we propose to take a critical control approach. To this end, we derive the transfer function representation of the PFC controller and yield a detailed design procedure. The effectiveness of the proposed method is confirmed through an experimental evaluation.

Keywords—Critical control, disturbance observer, mechatronics, motion control, predictive functional control, table drive systems.

I. Introduction

IN many industrial applications of positioning devices such as table drive systems, the so-called cascade control system is traditionally applied, which has a minor velocity loop with a PI or I-P controller and a major position loop with a P controller [3]. As a rule of thumb, the minor velocity loop should be designed so as to have faster dynamics than that of the major position loop. This design strategy sounds intuitive, but the tuning of these controllers gains is nontrivial, and inappropriate controller gains might result in poor closed-loop performance.

The predictive functional control (PFC) developed by Richalet *et al*. [1], [4], [5] is one of the model predictive control (MPC) schemes. The PFC is known for its good tracking performance and robustness against model uncertainties and disturbances. However, especially from mechatronics viewpoint, the speed of disturbance rejection is relatively slow in the PFC, though disturbances are asymptotically rejected. To overcome this drawback, Satoh *et al.* [6], [7] proposed a disturbance observer (DOB)-based PFC where the inner DOB feedback loop cancels disturbances immediately and the outer PFC loop achieves good reference tracking. We basically focus on the design and implementation of the DOB-based PFC in this paper.

Usually, the PFC does not handle constraints on controlled outputs. Although a few techniques for handling constraints have been proposed, they each have a drawback. For example, the technique proposed by Abu el Ata-Doss *et al.* [1] cannot handle constraints on manipulated variables and output variables in a unified manner, and a linear programing approach developed by Zhang *et al.* [13] increases on-line computational burden. We therefore propose to design the disturbance observer-based predictive functional control system as the critical control system (CCS) [11] in this paper. The CCS is defined as a control system which has responses required to be strictly within prescribed bounds for any exogenous inputs that are likely to occur in practice. Since the critical control systems design is based on an off-line computation, the proposed method does not increase the on-line computational burden. Also, all constraints are treated in a unified way.

The proposed control method, which is referred to as the disturbance observer-based predictive functional critical control (DOB-PFCC), is applied to a position control problem of a single axis table drive system. The effectiveness of the DOB-PFCC is checked through an experimental evaluation where constraints are imposed on the tracking error and controller output.

The organization of this paper is as follows. Section II provides a mathematical model of a single axis table drive system and a brief outline of the PFC, DOB and CSS where the transfer function representation of the PFC controller is given. A design procedure of the proposed control is also shown in Section II. Section III shows a detailed DOB-PFCC design for the single axis table drive system and experimental results. Section IV states conclusions.

II. Preliminaries

A. Notations and Definitions

Let $\mathbb{R}$, $\mathbb{R}_+$, $\mathbb{R}^n$, $\mathbb{Z}_+$, $\mathbb{Z}^n$ be the set of all real numbers, the set of all nonnegative real numbers, the set of all n-dimensional real vectors, the set of all nonnegative integers, and the set of all n-dimensional integer vectors, respectively. In addition, let $\mathcal{V}$ be the normed vector space of infinite sequences.

For an infinite sequence $x(k) : \mathbb{Z}_+ \to \mathbb{R}$, the l_∞ norm of $x(k)$ is defined by

$$\|x\|_\infty := \sup\{|x(k)| : k \in \mathbb{Z}_+\}, \tag{1}$$

and the l_1 norm of $x(k)$ is defined by

$$\|x\|_1 := \sum_{k=0}^{\infty} |x(k)|. \tag{2}$$

Finally, the difference of $x(k)$ is defined by $\Delta x(k) := x(k) - x(k-1)$.

T. Satoh, H. Hara and N. Saito are with the Department of Machine Intelligence and Systems Engineering, Akita Prefectural University, Yurihonjo, Akita, Japan (e-mail: {m15a009, tsatoh, naoki_saito} @akita-pu.ac.jp).
J. Nagase is with the Faculty of Science and Technology, Ryukoku University, Otsu, Shiga, Japan (e-mail: nagase@rins.ryukoku.ac.jp).
N. Saga is with the Department of Human System Interaction, Kwansei Gakuin University, Gakuen, Hyogo, Japan (e-mail: saga@kwansei.ac.jp).

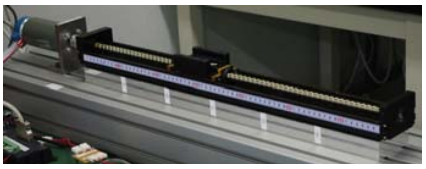

Fig. 1 Single axis table drive system

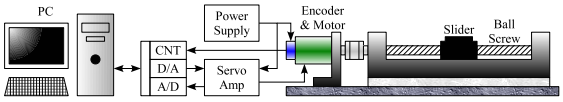

Fig. 2 Schematic diagram of experimental setup

B. Modeling of Table Drive Systems

Fig. 1 shows the external view of the single axis table drive system which is used in this paper. Also, Fig. 2 shows the schematic diagram of the experimental setup. As is clear from Fig. 2, the system is controlled by the semi-closed-loop control method. The core of this experimental apparatus is a single axis linear actuator, which is driven by an 80 Watt DC servo motor equipped with an optical encoder with the resolution of 1000 pulses/revolution. The DC motor is driven by a DC servo amplifier. The specifications of the linear actuator and DC motor are summarized in Table I. The encoder pulse is received by a 24-bit encoder counter board and counted by quad edge evaluation. The command signal to the DC servo amplifier is sent from a 12-bit digital-to-analogue converter, and the current monitor signal from the DC servo amplifier is received by a 12-bit analog-to-digital converter. The table drive system is controlled at the sample rate of 1 kHz.

We use the DC servo amplifier in the current control mode to command and control the motor torque instead of directly manipulating the motor current. Hence, on the assumption that the table drive system can be approximated by a one-inertia system, its equation of motion subject to friction torque is given by

$$\ddot{\theta}(t) = \frac{K_S}{J} e_a(t) - \frac{D}{J}\dot{\theta}(t) \tag{3}$$

where θ denotes the angle of the motor shaft, e_a is the command voltage to the DC servo amplifier, J is the equivalent moment of inertia, K_S is the conversion factor from the command voltage to the motor torque, and D is the viscous friction coefficients. In our experimental apparatus, the conversion factor is given by $K_S = 0.0801$ Nm/V, and the nominal value of the moment of inertia is identified as $J = 1.6928 \times 10^{-4}$ kg m^2 by using a standard system identification technique. We define the state vector and output variables as $(x_1\, x_2)^T := (\theta\, \dot{\theta})^T$ and $y := \theta$, respectively. Then the state-space description of the single axis table drive system is given by

$$\begin{cases} \begin{pmatrix} \dot{x}_1(t) \\ \dot{x}_2(t) \end{pmatrix} = \begin{pmatrix} 0 & 1 \\ 0 & -D/J \end{pmatrix} \begin{pmatrix} x_1(t) \\ x_2(t) \end{pmatrix} + \begin{pmatrix} 0 \\ K_S/J \end{pmatrix} e_a(t), \\ y(t) = \begin{pmatrix} 1 & 0 \end{pmatrix} \begin{pmatrix} x_1(t) \\ x_2(t) \end{pmatrix}. \end{cases} \tag{4}$$

TABLE I
SPECIFICATIONS OF TABLE DRIVE SYSTEM AND DC MOTOR

Description	Value	Description	Value
ball screw lead	10 mm	nominal voltage	24 V
stroke	500 mm	rated current	2.96 A
rail length	670 mm	rated torque	0.28 Nm
maximum rotational speed	500 mm/s	rated speed	1810 r/min

C. Predictive Functional Control

In this subsection, we give a brief overview of the *predictive functional control* (PFC). For more details of the PFC algorithm based on the state-space model, see, for example, S. Abu el Ata-Doss *et al.* [1].

Fig. 3 shows the basic concept of the PFC. Suppose that the current time is labeled as time step k. A *set-point trajectory* is defined as a command signal which the process output y_P should track, and the value of the set-point trajectory at the current time step is denoted by $c(k)$. Also shown is a *reference trajectory* denoted by y_R. This trajectory starts at the current process output $y_P(k)$ and defines a desired trajectory along which the process output y_P should follow. On the reference trajectory, there are a few *coincidence points* on which the performance index is defined so that the process output y_P will coincide with the reference trajectory y_R. As an example, three coincidence points are shown in Fig. 3. The optimal control input trajectory is then computed on the basis of the predicted output. Once we have computed a future control input trajectory, we apply only the first element to the process. At the next time step, we repeat the whole cycle from the definition of the reference trajectory to the application of the first element of the optimal control input trajectory. We call this way of control a *receding horizon control*.

Next, we show the basic PFC algorithm. Now assume that the plant is stable and has the time delay of L and that the sampling period is T_s. The development of the PFC algorithm is based on the following SISO discrete-time linear state-space model of the plant:

$$\begin{cases} x_M(k+1) = A_M x_M(k) + B_M u(k), \\ y_M(k) = C_M x_M(k) \end{cases} \tag{5}$$

where $x_M \in \mathbb{R}^n$ is the state vector, $u \in \mathbb{R}$ is the control input, $y_M \in \mathbb{R}$ is the model output, respectively. Here, the

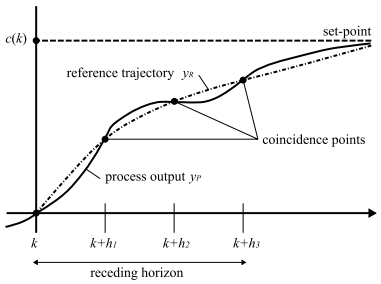

Fig. 3 Concept of the predictive functional control

model output $y_M(k)$ is used to predict the future plant output $\hat{y}_P(k+d)$ where $d \in \mathbb{Z}$ is defined as the nearest integer to L/T_s. Assume that the following condition holds:

$$\det \begin{pmatrix} A_M - I & B_M \\ C_M & 0 \end{pmatrix} \neq 0. \tag{6}$$

Then the reference trajectory is defined as follows:

$$y_R(k+d+i) := c(k+d+i) - \alpha^i \left(c(k+d) - \hat{y}_P(k+d) \right), \tag{7}$$

where $\alpha \in \mathbb{R}$ is a parameter which adjusts the approaching ratio of the reference trajectory to the set-point ($0 < \alpha < 1$). In this paper, we choose the parameter α as $\alpha = e^{-3T_s/T_{\mathrm{CLTR}}}$ along with the following three coincidence points:

$$\begin{pmatrix} h_1 & h_2 & h_3 \end{pmatrix} = \begin{pmatrix} \dfrac{T_{\mathrm{CLTR}}}{3T_s} & \dfrac{T_{\mathrm{CLTR}}}{2T_s} & \dfrac{T_{\mathrm{CLTR}}}{T_s} \end{pmatrix} \tag{8}$$

where $T_{\mathrm{CLTR}} \in \mathbb{R}$ is constant and called the *desired closed-loop time response*. The performance index is defined as the quadratic sum of the errors between the predicted process output $\hat{y}_P$ and the reference trajectory y_R as follows:

$$J(k) := \sum_{j=1}^{n_h} \left\{ \hat{y}_P(k+d+h_j) - y_R(k+d+h_j) \right\}^2 \tag{9}$$

where $h_j \in \mathbb{Z}$ $(j = 0, 1, \ldots, h)$ and $n_h \in \mathbb{Z}$ are respectively the coincidence time point and the number of coincidence points. In the PFC, the future control input computed at each sampling instant is assumed to be the sum of weighted basis functions, and a time-dependent polynomial basis is usually employed. Then the optimal control input that minimizes the performance index (9) is given by

$$\begin{aligned} u(k) = k_0 \left\{ c(k+d) - y_P(k) \right\} \\ + \tilde{\nu}_x^T x_M(k) + \tilde{\nu}_{xd}^T x_M(k-d) \end{aligned} \tag{10}$$

where $k_0 \in \mathbb{R}$, $k_m \in \mathbb{R}$, $\tilde{\nu}_x \in \mathbb{R}^n$ and $\tilde{\nu}_{xd} \in \mathbb{R}^n$ are respectively given by

$$k_0 = \nu^T \begin{pmatrix} 1-\alpha^{h_1} \\ \vdots \\ 1-\alpha^{h_{n_h}} \end{pmatrix}, \ \tilde{\nu}_x = -\begin{pmatrix} C_M \left(A_M^{h_1} - \alpha^{h_1} I \right) \\ \vdots \\ C_M \left(A_M^{h_{n_h}} - \alpha^{h_{n_h}} I \right) \end{pmatrix}^T \nu, \tilde{\nu}_{xd} = -\begin{pmatrix} \left(\alpha^{h_1} - 1 \right) C_M \\ \vdots \\ \left(\alpha^{h_{n_h}} - 1 \right) C_M \end{pmatrix}^T \nu. \tag{11}$$

In (11), $\nu \in \mathbb{R}^{n_h}$ is given by

$$\nu = \begin{pmatrix} y_B(h_1) & \cdots & y_B(h_{n_h}) \end{pmatrix}^T \left(\sum_{j=1}^{n_h} y_B(h_j) \, y_B(h_j)^T \right)^{-1} U_B(0) \tag{12}$$

where $y_B(h_j) = \begin{pmatrix} y_{B_1}(h_j) & \cdots & y_{B_{n_B}}(h_j) \end{pmatrix}^T \in \mathbb{R}^{n_B}$ and $U_B(0) = \begin{pmatrix} 1 & 0 & \cdots & 0 \end{pmatrix}^T \in \mathbb{Z}^{n_B}$. Here, $y_{B_l}(i) \in \mathbb{R}$ is the forced response to the basis function of the form i^{l-1} $(l = 1, 2, \ldots, n_B)$.

D. Transfer Function representation of PFC Controller

Since the optimal control law in (10) is linear and time-invariant, it is possible to derive the transfer function representation of the PFC controller as stated in the following theorem.

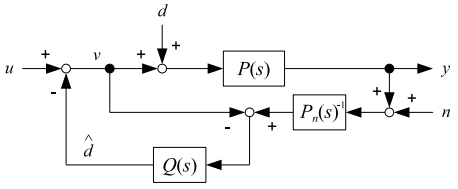

Fig. 4 Structure of the disturbance observer

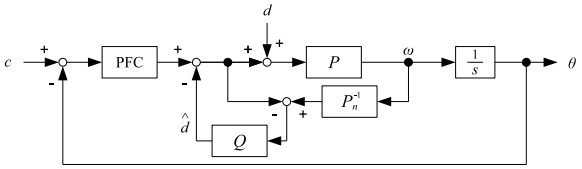

Fig. 5 Block diagram of DOB-based PFC for single axis servo system

Theorem 1. *Let us introduce the following notation:*

$$\left(\begin{array}{c|c} A & B \\ \hline C & D \end{array} \right) = C(zI - A)^{-1} B + D. \tag{13}$$

Then, the pulse transfer function of the PFC controller is given by

$$C(z) = \left(\begin{array}{c|c} A^\natural & B^\dagger \\ \hline C^\natural & k_0 \end{array} \right) \tag{14}$$

where

$$\begin{aligned} A^\natural &:= \begin{pmatrix} 0 & I & 0 & \cdots & 0 \\ 0 & 0 & I & \cdots & 0 \\ \vdots & \vdots & \vdots & \ddots & \vdots \\ 0 & 0 & 0 & \cdots & I \\ B_M \tilde{\nu}_{xd}^T & 0 & 0 & \cdots & A_M + B_M \tilde{\nu}_x^T \end{pmatrix} \in \mathbb{R}^{n(d+1) \times n(d+1)}, \\ B^\dagger &:= \begin{pmatrix} 0 \\ \vdots \\ 0 \\ B_M k_0 \end{pmatrix} \in \mathbb{R}^{n(d+1) \times 1}, \ C^\natural := \begin{pmatrix} \tilde{\nu}_{xd}^T & 0 & \cdots & \tilde{\nu}_x^T \end{pmatrix} \in \mathbb{R}^{1 \times n(d+1)}. \end{aligned} \tag{15}$$

Moreover, when $d = 0$, the resulting pulse transfer function is given by

$$C(z) = \left(\begin{array}{c|c} A_M + B_M \nu_x^T & B_M k_0 \\ \hline \nu_x^T & k_0 \end{array} \right) \tag{16}$$

where

$$\nu_x := -\begin{pmatrix} C_M \left(A_M^{h_1} - I \right) \\ \vdots \\ C_M \left(A_M^{h_{n_h}} - I \right) \end{pmatrix}^T \nu \in \mathbb{R}^n. \tag{17}$$

Proof: Omitted. ■

The above result serves as a foundation for the design of the DOB-PFCC.

E. Disturbance Observer-based Predictive Functional Control

A brief outline of the disturbance observer-based predictive functional control [6], [7] is given in this subsection.

The *disturbance observer* (DOB) has the structure depicted in Fig. 4 where $P(s)$ is the transfer function of the real plant, $P_n(s)$ is the nominal model of the plant, and $Q(s)$ is a

proper and stable low-pass filter (LPF). The nominal model $P_n(s)$ is supposed to be minimum-phase in the following. On the assumption that disturbances acting on the system, modeling errors and nonlinearities can be regarded as an equivalent disturbance d at the plant input, the DOB computes the estimate $\hat{d}$ of the current disturbance d, which is subtracted from the input u to cancel the disturbance.

When the plant has no unstable zeros, the LPF $Q(s)$ can be selected as [9]

$$Q(s) = \frac{1 + \sum_{m=1}^{n_q-\rho_q} f_m s^m}{1 + \sum_{m=1}^{n_q} f_m s^m} \tag{18}$$

where $n_q \in \mathbb{Z}$, $\rho_q \in \mathbb{Z}$ and $f_m \in \mathbb{R}$ are respectively the order of $Q(s)$, the relative degree of $Q(s)$ and unknown coefficients to be determined. To make $Q(s) P_n(s)^{-1}$ proper, ρ_q must be chosen as $\rho_q \geqslant \rho_P$ where $\rho_P \in \mathbb{Z}$ is the relative degree of $P_n(s)$.

Various types of analogue filters can be utilized to realize $Q(s)$, and in many cases, the Butterworth and the binomial LPFs are used. More specifically, the Butterworth filter is a reasonable option when $n_q = \rho_q$, which means that the degree of the numerator polynomial of $Q(s)$ is 0. Otherwise, the binomial filter of the following form is useful:

$$Q(s) = \frac{1 + \sum_{m=1}^{n_q-\rho_q} a_m \left(s\tau_{n_q}\right)^m}{1 + \sum_{m=1}^{n_q} a_m \left(s\tau_{n_q}\right)^m} \tag{19}$$

where $a_m\,(m = 1, 2, \ldots, n_q)$ are the binomial coefficients (*i.e.*, $a_m = n_q!/m!(n_q - m)!$) and τ_{n_q} is a design variable to be determined.

The disturbance observer is assumed to be placed in the velocity loop. Hence, if $d = 0$, the block diagram of the disturbance observer-based predictive functional control system for the table drive system is shown as Fig. 5 where the transfer function of the PFC controller is given by (16).

F. Critical Control

Critical systems are defined as control systems that have responses required to be strictly within the prescribed bounds to any inputs that are likely to occur in practice [11].

Let $w \in \mathbb{R}$ and $z(w) \in \mathbb{R}^m$ respectively denote an exogenous input to the system, and the response vector of the closed-loop system is defined by

$$z(w) := \begin{pmatrix} z_1(w) & z_2(w) & \cdots & z_m(w) \end{pmatrix}^T. \tag{20}$$

Suppose that w belongs to a predefined set $\mathcal{W}$ and that $w(k) = 0$ for $k \leqslant 0$. The set $\mathcal{W}$ is called the *possible set* [12]. The control of critical systems, which is referred to as *critical control*, is then formulated as

$$|z_i(k, w)| \leqslant \varepsilon_i, \quad k \in \mathbb{Z}_+,\ w \in \mathcal{W},\ i = 1, 2, \ldots, m. \tag{21}$$

where $\varepsilon_i \in \mathbb{R}_+$ is the largest tolerable value of the absolute response $|z_i(k, w)|$. (21) can be rewritten as

$$\hat{z}_i(\mathcal{W}) \leqslant \varepsilon_i, \quad i = 1, 2, \ldots, m, \tag{22}$$

where $\hat{z}_i(\mathcal{W})$ is defined by

$$\hat{z}_i(\mathcal{W}) := \sup\{\|z_i(w)\|_\infty : w \in \mathcal{W}\}. \tag{23}$$

Hence, the critical control problem is stated as follows: *find an internally stabilizing controller that ensures the criteria* (22) *for any input that belongs to a known input set* $\mathcal{W}$.

The choice of the possible set $\mathcal{W}$ is essential for the design of critical control systems. Throughout this paper, the following possible set is used:

$$\mathcal{W}_\infty(\mathcal{M}, \mathcal{D}) := \{w \in \mathcal{V} : \|w\|_\infty \leqslant \mathcal{M},\ \|\Delta w\|_\infty \leqslant \mathcal{D}\}. \tag{24}$$

The possible set (24) contains magnitude-and-rate-limited inputs, and it excludes inputs with infinite rate of change such as the unit step function.

In general, we must rely on a complex numerical analysis or optimization to compute the value of $\hat{z}_i(\mathcal{W}_\infty(\mathcal{M}, \mathcal{D}))$ (see, for example, Lane [2] or Silpsrikul and Arunsawatwong [8]). However, the following relationship can be derived:

$$\hat{z}_i(\mathcal{W}_\infty(\mathcal{M}, \mathcal{D})) \leqslant \mathcal{M}\left|\lim_{k\to\infty} z_i(k, 1)\right| + \mathcal{D}\left\|z_i(1) - \lim_{k\to\infty} z_i(k, 1)\right\|_1 \tag{25}$$

where 1 is the unit step function, and $z_i(k, 1)$ is the unit step response at k. Therefore, we can utilize the right-hand side of (25) as a useful approximation of $\hat{z}_i(\mathcal{W}_\infty(\mathcal{M}, \mathcal{D}))$. The relationship in (25) is a natural consequence of the similar approximation derived in continuous-time domain [10].

It should be noted that, if $\lim_{k\to\infty} z_i(k, 1) = 0$, the possible set in (24) may be replaced with

$$\mathcal{W}_\infty(\mathcal{D}) := \{w \in \mathcal{V} : \|\Delta w\|_\infty \leqslant \mathcal{D}\}, \tag{26}$$

and $\hat{z}_i(\mathcal{W}_\infty(\mathcal{D}))$ is given by

$$\hat{z}_i(\mathcal{W}_\infty(\mathcal{D})) = \mathcal{D}\|z_i(1)\|_1, \tag{27}$$

which means that the supremum absolute value is determined only by the rate of change $\mathcal{D}$ without approximation. In this case, no complex numerical analysis or optimization is required to compute $\hat{z}_i(\mathcal{W}_\infty(\mathcal{D}))$.

G. Design Procedure of DOB-PFCC System

In many cases, critical systems are designed by searching a number of adjustable parameters directly. For example, coefficients of the denominator and numerator polynomials in the controller transfer function, or the closed-loop poles are numerically searched to meet the design criteria in (22). On the other hand, PFC has only one design parameter: the desired closed-loop time response T_{CLTR}. Hence, the design procedure of the proposed DOB-PFCC system design is summarized as follows:

Step 1. Specify the desired closed-loop time response T_{CLTR}.
Step 2. Calculate the closed-loop transfer functions from w to $z_i\,(i = 1, 2, \ldots, m)$ using the plant model $P(z)$ and the PFC controller transfer function $C(z)$.
Step 3. Check whether all of the closed-loop poles are inside the unit circle. If so, proceed to Step 4.; otherwise return to Step 1.
Step 4. Compute the the upper bound of $\hat{z}_i(\mathcal{W})$ $(i = 1, 2, \ldots, m)$ given in the right-hand side of (25).
Step 5. Check whether the design criteria in (22) are satisfied. If so, the design is completed; otherwise, return to Step 1.

TABLE II
UPPER BOUND OF THE SUPREMUM PEAK RESPONSE

T_{CLRT}	tracking error (rad)	controller output (V)
0.05	0.272	1.117
0.08	0.434	0.684
0.10	0.542	0.542
0.30	1.605	0.169
0.50	2.644	0.101

III. Design and Experiment

A. Design of Disturbance Observer and PFC Controller

First, we design a Q-filter in the disturbance observer. From the state-space realization of the plant in (4), the nominal transfer function from the command voltage e_a to the angular velocity $\dot{\theta}$ is given by

$$P_n(s) = \frac{K_s}{Js + D} = \frac{473.2}{s + 3.32}. \tag{28}$$

It follows from (28) that the relative degree ρ_q of the Q-filter must be greater than or equal to 1. So we assume that $\rho_q = 1$ hereafter. When n_I is taken to be 2, the order of the Q-filter is $n_q = n_I + \rho_q - 1 = 2$. We therefore design a second-order filter with the relative degree of 1. According to the numerical design procedure used in Satoh *et al.* [6], we obtained the following second-order binomial filter $Q(s)$ with a cut-off frequency of 45 Hz:

$$Q(s) = \frac{150.38\,(s + 37.59)}{(s + 75.19)^2}. \tag{29}$$

Secondly, we define the possible set $\mathcal{W}$ and the design specification. We use the following possible set in this experiment:

$$\mathcal{W}_\infty(10, 0.01) := \{w \in \mathcal{V} : \|w\|_\infty \leqslant 10,\ \|\Delta w\|_\infty \leqslant 0.01\}. \tag{30}$$

Let us suppose that we have two responses to be bounded, namely, the tracking error z_1 and the PFC controller output z_2. We also assume that the purpose of control here is to keep the two responses within the following bounds:

$$\begin{cases} \hat{z}_1(\mathcal{W}_\infty(10, 0.01)) \leqslant 0.5 \text{ rad}, \\ \hat{z}_2(\mathcal{W}_\infty(10, 0.01)) \leqslant 1 \text{ V}. \end{cases} \tag{31}$$

Next, we design an admissible controller by adjusting the closed-loop response time T_{CLRT}. It is obvious from **Theorem 1** that the resulting PFC controller varies as T_{CLRT} is changed, and the upper bound of $\hat{z}_i(\mathcal{W}_\infty(10, 0.01))$ (*i.e.*, the right-hand side of (25)) is hence changed as shown in Table II. Moreover, Table II shows that, as T_{CLRT} becomes larger, the worst-case tracking error increases, whereas the worst-case PFC controller output decreases. It can be seen from Table II that the design specification in (31) is satisfied when $T_{\mathrm{CLRT}} = 0.08$, so that the PFC controller is designed by using this value. The pulse transfer function of the controller is then given by

$$C_{0.08}(z) = \frac{4.015\,(z - 0.997)}{z - 0.918}. \tag{32}$$

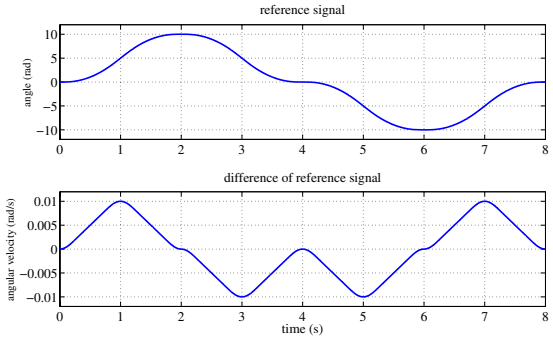

Fig. 6 Reference signal and its difference

When $C_{0.08}(z)$ is used, for *any* reference input $w \in \mathcal{W}_\infty(10, 0.01)$, the tracking error and controller output are always kept within the bounds 0.434 rad and 0.684 V, respectively.

We mention that $\lim_{k\to\infty} z_i(k, 1) = 0$ $(i = 1, 2)$ in this control system. Hence, the possible set $\mathcal{W}_\infty(\mathcal{D})$ given in (26) can be used instead of $\mathcal{W}_\infty(\mathcal{M}, \mathcal{D})$. In that case, Table II shows not the upper bound but the exact value of the supremum peak response for any input in $\mathcal{W}_\infty(0.01)$.

B. Experimental Evaluation

One of the reference inputs that belong to the possible set $\mathcal{W}_\infty(10, 0.01)$ can be constructed by connecting a number of modified trapezoidal curves as shown in Fig. 6. This reference input is clearly an element in the possible set $\mathcal{W}_\infty(10, 0.01)$ since $|w(k)| \leqslant 10$ and $|\Delta w(k)| \leqslant 0.01$ for $k \geqslant 0$.

Fig. 7 shows the experimental result of the DOB-PFCC system where the Q-filter in (29) and the controller in (32) are combined together. We can confirm that both the tracking error z_1 and the PFC controller output z_2 fulfill the requirements in (31). The tracking error is very close to the upper bound 0.434 rad and thus to the design requirement 0.5 rad. On the other hand, the controller output z_2 is far from the upper bound 0.684 V and hence from the design specification 1 V. So, the design is tight from the point of view of the tracking error, but conservative from the perspective of the controller output.

For purposes of comparison, the experimental results using other T_{CLRT} are shown in Fig. 8 and Fig. 9 where T_{CLRT} is 0.3 and 0.5, respectively. The PFC controllers corresponding to these values are given as follows:

$$C_{0.3}(z) = \frac{0.310\,(z - 0.997)}{z - 0.977}, \tag{33}$$

$$C_{0.5}(z) = \frac{0.120\,(z - 0.997)}{z - 0.985}. \tag{34}$$

We know from Table II that we cannot ensure the bound $\hat{z}_1(\mathcal{W}_\infty(10, 0.01)) \leqslant 0.5$ rad for $T_{\mathrm{CLRT}} = 0.3$ and 0.5. In fact, the tracking error violates the constraint as shown in Fig. 8 and Fig. 9.

It should be emphasized here that z_2 is not the overall control effort but just the PFC controller output. The overall

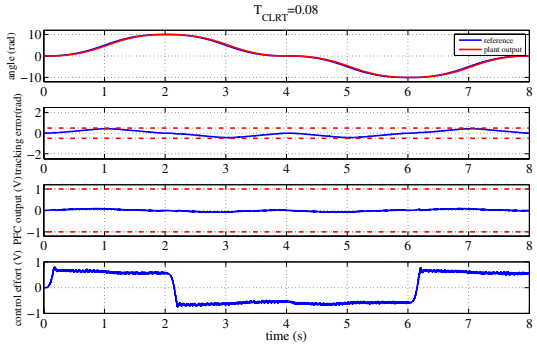

Fig. 7. Experimental results ($T_{\mathrm{CLRT}} = 0.08$)

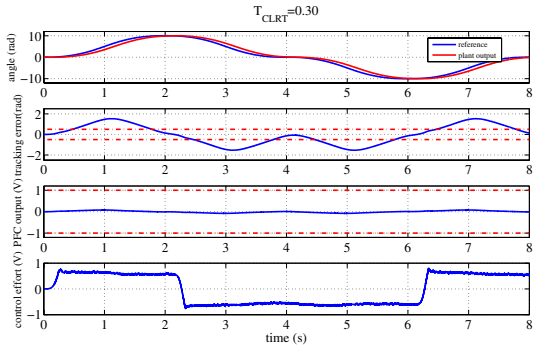

Fig. 8. Experimental results ($T_{\mathrm{CLRT}} = 0.3$)

control effort, which is the sum of the DOB output and the PFC controller output, should be bounded in practice. In the presence of unmodeled dynamics, uncertainties and parasitic effects such as friction, the overall control effort differs from the PFC controller output since the disturbance observer functions so as to compensate for the plant-model mismatch (see the bottom figures in Fig. 7, Fig. 8 and Fig. 9). Unfortunately, the proposed design method cannot take account of the overall control effort directly. For this specific design example, however, we are able to evaluate the overall control effort in an ad hoc manner as follows. Fig. 7, Fig. 8 and Fig. 9 suggest that the DOB output is almost the same irrespective of the value of T_{CLRT}. So, measuring the DOB output for the reference input beforehand, we can estimate the maximum absolute value of the DOB output. Then the upper bound of the overall control effort can be approximated by the sum of the estimate and $\hat{z}_2\left(\mathcal{W}_\infty\left(10, 0.01\right)\right)$.

IV. Conclusions

We have presented a disturbance observer-based predictive functional critical control method for the position control of a table drive system. The proposed method can handle constraints on the responses without on-line optimization, so that the advantage of PFC is still retained. The experimental results show that the designed DOB-PFCC controller satisfies the constraints on the tracking error and PFC controller output.

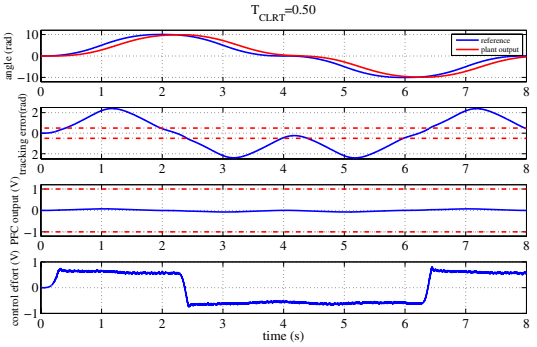

Fig. 9. Experimental results ($T_{\mathrm{CLRT}} = 0.50$)

Acknowledgment

This work was supported by the Japan Society for the Promotion of Science under Grant-in-Aid for Scientific Research (C) 25420191.

References

[1] S. Abu el Ata-Doss, P. Fiani and J. Richalet, "Handling input and state constraints in predictive functional control," *Proc. of the 30th Conference on Decision and Control*, pp. 985-990, Brighton, England, 1991.

[2] P. G. Lane, "Design of control systems with inputs and outputs satisfying certain bounding conditions," Ph. D. thesis, University of Manchester Institute of Science and Technology, Manchester, U.K., 1992.

[3] A. Matsubara, *Design and Control of Precision Positioning and Feed Drive systems.* Tokyo, Japan: Morikita Publishing, 2008. (in Japanese)

[4] J. Richalet, S. Abu el Ata-Doss, C. Arber, H.B. Kuntze, A. Jacubasch and W. Schill, "Predictive functional control: application to fast and accurate robot," *Proceedings of IFAC 10th World Congress*, Munich, Germany, pp. 251-258, 1987.

[5] J. Richalet and D. O'donovan, *Predictive Functional Control: Principles and Industrial Applications.* London, England: Springer-Verlag, 2009.

[6] T. Satoh, K. Kaneko and N. Saito, "Improving tracking performance of predictive functional control using disturbance observer and its application to table drive systems," *International Journal of Computers Communications & Control*, vol. 7, no. 3, pp. 550-564, 2012.

[7] T. Satoh, N. Saito and N. Saga, "Predictive functional control with disturbance observer for pneumatic artificial muscle actuator," *Proceeding of the 1st International Conference on Applied Bionics and Biomechanics*, Venice, Italy, no page number, 2010.

[8] W. Silpsrikul and S. Arunsawatwong, "Computation of peak output for inputs restricted in L_2 and L_∞ norms using finite difference schemes and convex optimization," *International Journal of Automation and Computing*, vol. 6, no. 1, pp. 7-13, 2009.

[9] T. Umeno and Y. Hori, Robust speed control of DC servomotors using modern two-degrees-of-freedom controller design, *IEEE Transactions on Industrial Electronics*, vol. 38, no. 5, pp. 363-368, 1991.

[10] V. Zakian, "New formulation for the method of inequalities," *Proceedings, IEE*, vol. 126, pp. 579-584, 1979.

[11] V. Zakian, "Critical systems and tolerable inputs," *International Journal of Control*, vol. 49, no. 4, pp. 1285-1289, 1989.

[12] V. Zakian, "Perspectives on the principle of matching and the method of inequalities," *International Journal of Control*, vol. 65, no. 1, pp. 147-175, 1996.

[13] R. Zhang, A. Xue, S. Wang and J. Zhang, "An improved state-space model structure and a corresponding predictive functional control design with improved control performance," *International Journal of Control*, vol. 85, no. 8, pp. 1146-1161, 2012.